Available online at website: https://journal.bcrec.id/index.php/bcrec

Bulletin of Chemical Reaction Engineering & Catalysis, 21 (3) 2026, 600-610

Original Research Article

Effect of Calcination Temperature on Structural Properties and Photocatalytic Activity of TiO_2/Vermiculite Composite for Methylene Blue Degradation

Nam Duy Dao[1]*, Trang Vu Minh[1], Hai Trung Huynh[2], Ha Thi Thu Vu[3]*

[1]*School of Chemistry and Life Science, Hanoi University of Science and Technology, 1 Dai Co Viet, Bach Mai, Hanoi, Vietnam.*

[2]*School of Materials Science and Engineering, Hanoi University of Science and Technology, 1 Dai Co Viet, Bach Mai, Hanoi, Vietnam.*

[3]*National Key Laboratory for Petrochemical and Refinery Technology, 2 Pham Ngu Lao Street, Cua Nam, Hanoi, Vietnam.*

Received: 13th May 2026; Revised: 18th June 2026; Accepted: 19th June 2026
Available online: 22th June 2026; Published regularly: October 2026

Abstract

This study investigated the effect of calcination temperature on the structural properties and photocatalytic performance of TiO_2/vermiculite (TiO_2/ver) composites for methylene blue (MB) degradation. The TiO_2/ver composites were synthesized via a one-step sol-gel method using titanium (IV) isopropoxide (TTIP) as the precursor, followed by calcination at 450, 600 and 800 °C. Structural characterization by X-ray diffraction (XRD) revealed that the anatase phase predominance in samples calcined at 450 and 600 °C, whereas partial transformation to rutile occurred at 800 °C. Scanning electron microscopy (SEM) showed that increasing calcination temperature promoted particle growth and agglomeration. Fourier-transform infrared (FT-IR) analysis revealed the coexistence of characteristic Ti-O-Ti and Si-O vibrations and indicated possible interfacial interactions between TiO_2 and the vermiculite support through a shift the Si-O stretching band. Textural analysis demonstrated a progressive decrease in specific surface area with increasing calcination temperature, suggesting thermally induced pore collapse and crystallite growth. Photocatalytic experiments demonstrated that the sample calcined at 450 °C (V-450) exhibited the highest photocatalytic activity, achieving complete MB degradation within 90 min under the optimal conditions of a catalyst dosage of 1.0 $g.L^{-1}$, an initial MB concentration of 10 $mg.L^{-1}$ and pH of 7. Kinetic analysis showed that the degradation followed pseudo-first-order kinetics. The superior performance of the V-450 was attributed to the optimal balance between crystallinity, specific surface area and phase composition. These findings highlight the critical role of calcination temperature in tuning the structure-activity relationship of TiO_2/ver composites for photocatalytic wastewater treatment applications.

Keywords: TiO_2/vermiculite; photocatalysis; methylene blue; calcination temperature; wastewater treatment

How to Cite: Dao Duy, N., Vu Minh, T., Huynh Trung, H., Thu Vu, H. T. (2026). Effect of Calcination Temperature on Structural Properties and Photocatalytic Activity of TiO_2/Vermiculite Composite for Methylene Blue Degradation. *Bulletin of Chemical Reaction Engineering & Catalysis*, 21 (3), 600-610. (DOI: 10.9767/bcrec.20736)

Permalink/DOI: https://doi.org/10.9767/bcrec.20736

1. Introduction

Titanium dioxide (TiO_2) is one of the most extensively investigated photocatalytic materials for environmental remediation because of its strong oxidative capability, high chemical stability, low cost, and relatively low toxicity [1-3]. Nevertheless, the practical application of TiO_2 nanoparticles in suspension systems remains constrained by several intrinsic limitations, including nanoparticle aggregation, which reduces the effective surface area, and the difficulty of catalyst recovery after treatment [4-6]. In addition, the relatively low adsorption capacity of TiO_2 toward organic contaminants often restricts overall photocatalytic efficiency, particularly in dilute aqueous solutions [7].

To overcome these limitations, immobilizing TiO_2 onto suitable support materials has emerged

* Corresponding Authors.
Email: nam.daoduy@hust.edu.vn (N.D. Dao),
ptntd2004@yahoo.fr. (H.T.T. Vu)

as an effective strategy for improving nanoparticle dispersion, suppressing aggregation, enhancing adsorption capacity and facilitating catalyst recovery [8]. An ideal support material should possess a high specific surface area and suitable adsorption properties to concentrate pollutants near photocatalytic active sites. Simultaneously, the adsorption strength should remain moderate to ensure efficient diffusion and mass transfer of adsorbed molecules toward the TiO_2 surface, where photocatalytic degradation occurs [9].

Among various support materials, clay minerals have attracted considerable attention because of their layered structures, adsorption capability, low cost and environmental compatibility [4,8]. Various clay-based supports, including kaolinite, bentonite, halloysite and vermiculite, have been investigated for photocatalytic applications following physical or chemical modifications such as acid activation, thermal treatment, ion exchange, pillaring and surface functionalization [8,10-13]. These modification strategies can improve surface area, porosity, interlayer accessibility, and dispersion of photocatalytic nanoparticles, thereby enhancing photocatalytic activity and catalyst stability [5,14].

Compared with many conventional clay minerals, vermiculite exhibits several distinctive properties that make it particularly attractive as a photocatalyst support material [11]. More importantly, vermiculite exhibits unique thermal expansion behavior during heat treatment due to the rapid release of interlayer water molecules [15]. This exfoliation process can generate a more porous and expanded layered structure, which is beneficial for TiO_2 dispersion, pollutant diffusion and mass transfer during photocatalytic reactions [16]. Such structural characteristics make vermiculite a promising support material for thermally treated photocatalytic systems.

Recent studies have demonstrated that vermiculite-based composites can significantly enhance photocatalytic degradation efficiency through the synergistic combination of adsorption and photocatalysis [11,17]. Vermiculite-supported TiO_2 materials have shown improved removal performance toward organic pollutants because the layered structure of vermiculite facilitates pollutant enrichment near photocatalytic active sites while simultaneously suppressing nanoparticle aggregation [11,18]. Nevertheless, the structural evolution of vermiculite during calcination and its influence on photocatalytic behavior remain insufficiently understood.

The sol–gel method is widely employed for the synthesis of TiO_2 nanoparticles and TiO_2-based composites because it enables effective control of hydrolysis- condensation reactions, particle growth, and TiO_2 dispersion on support materials [11]. Previous studies have shown that the physicochemical properties of sol-gel derived TiO_2, including crystallinity, morphology, pore structure and photocatalytic activity are highly sensitive to calcination temperature [18-20]. In supported photocatalytic systems, calcination temperature strongly affects crystal phase composition, crystallite size, particle aggregation, surface area and pore structure, all of which directly influence photocatalytic performance [20].

Although numerous studies have investigated TiO_2/clay photocatalysts, most have primarily focused on compositional modification or pollutant degradation efficiency. In contrast, systematic investigations into the calcination-governed structure-activity relationship of TiO_2/vermiculite composites remain limited. In particular, the role of thermally expandable vermiculite in controlling TiO_2 phase evolution, pore development, and photocatalytic behavior during calcination has not been comprehensively clarified.

Therefore, the present study aims to investigate the influence of calcination temperature on the structural characteristics and photocatalytic performance of TiO_2/ver composites synthesized via a one-step sol-gel method. The composites were calcined at 450, 600 and 800°C and characterized using X-ray diffraction (XRD), scanning electron microscopy (SEM), Fourier-transform infrared spectroscopy (FT-IR), and Brunauer-Emmett-Teller (BET) surface area analysis. Their photocatalytic activity toward methylene blue degradation was systematically evaluated under different operating conditions. The findings provide new insights into the structure-activity relationship of vermiculite supported TiO_2 photocatalysts and contribute to the development of efficient and low-cost photocatalysts materials for wastewater treatment applications.

2. Materials and Methods

2.1. Materials

All chemicals used in this study were of analytical grade and used without further purification. Titanium(IV) isopropoxide (TTIP, 97%), ethanol (EtOH, ≥99%), hydrochloric acid (HCl, 37%), sodium hydroxide (NaOH, ≥98%), and methylene blue (MB) were purchased from Sigma-Aldrich. Commercial TiO_2 nanoparticles (99.9%, average particle size 25 nm, Degussa) were used as a reference photocatalyst. Commercial vermiculite was employed as support material.

According to the supplier's specifications, vermiculite exhibited a bulk density of 104–113 kg/m^3, a specific surface area of 8–9 m^2/g, a water absorption capacity of 500–700 $L.m^{-3}$ and a cation exchange capacity of approximately 150 meq/100 g. The pH of vermiculite in aqueous suspension

was approximately 7.0. Its major chemical composition consisted of SiO_2 (47.82%), Al_2O_3 (7.93%), MgO (19.38%), Fe_2O_3 (5.13%). Deionized water with a resistivity of 18 MΩ.cm was used throughout all experiments.

2.2. Catalyst Synthesis

Raw vermiculite was initially ground using an agate mortar to obtain a uniform powder, followed by sieving through a 140 µm standard sieve (Chung Gye Sang Gong Sa, Korea). The collected fraction (<140 µm) was used as the support material for catalyst synthesis. TiO_2 was synthesized via a sol–gel method and immobilized onto the vermiculite. Briefly, 20 mL of ethanol was introduced into a 250 mL beaker and stirred at 200 rpm for 15 min at room temperature. Subsequently, 10 mL of TTIP was added dropwise under continuous stirring and maintained for an additional 15 min to obtain a homogeneous precursor solution. Deionized water was then added dropwise at a controlled rate of approximately 40 drops.min^{-1} using a separatory funnel to initiate hydrolysis. After complete addition, the mixture was continuously stirred for 30 min to promote hydrolysis and condensation reactions. The resulting suspension was subsequently aged at room temperature until gel formation occurred.

The obtained solid product was separated by vacuum filtration using a 0.45 µm membrane filter (Schleicher & Schuell, Germany) and thoroughly washed with deionized water to remove residual alcohol, unreacted precursor species, and soluble by-products generated during the sol-gel process. The washing process continued until the filtrate reached near neutral pH and no visible turbidity was observed, indicating effective removal of residual impurities. The obtained material was then dried at 120 °C for 2 h.

After drying, the sample was gently ground using an agate mortar and subsequently calcined in air at different temperatures (450, 600, and 800 °C) for 2 h with a heating rate of 5 °C.min^{-1}. After calcination, the samples were allowed to cool naturally inside the furnace and then ground to obtain uniform TiO_2/vermiculite composites, denoted as V-x, where x represents the calcination temperature.

2.3. Characterizations

The crystalline structure and phase composition of the synthesized materials were analyzed using X-ray diffraction (XRD) on an AERIS diffractometer with Cu-Kα radiation (λ_1 = 1.5406 Å, λ_2 = 1.5444 Å), operated at 40 kV and 15 mA. The diffraction patterns were recorded over a 2θ range of 20–80° at room temperature. The surface morphology and particle size distribution was examined using field-emission scanning electron microscopy (FESEM, JEOL JEM-1010, Tokyo, Japan). Elemental composition was determined by energy-dispersive X-ray spectroscopy (EDS) using a GENESIS system. Textural properties, including specific surface area, pore volume, and pore size distribution, were determined by N_2 adsorption-desorption isotherms at 77 K using the Brunauer-Emmett-Teller (BET) method. Prior to analysis, the samples were degassed under vacuum at 120 °C for 6 h. Fourier-transform infrared (FT-IR) spectroscopy was employed to investigate the surface functional groups and possible interactions between TiO_2 and the vermiculite support. FT-IR spectra were recorded using a Thermo Fisher Scientific FT-IR spectrometer in the wavenumber range of 4000-400 cm^{-1} at room temperature. Prior to analysis, the samples were finely ground and dried to minimize interference from physically adsorbed moisture.

2.4. Photocatalytic Experiments

The photocatalytic activity of the catalysts was evaluated using methylene blue (MB) as a model organic pollutant. The experiments were conducted under irradiation from a high-pressure mercury lamp (OSRAM, 150 W) as illustrated in Figure 1. The average light intensity was measured to be 5.0 mW.cm^{-2} using an advanced light meter (Geneq, model 840022). The reaction system consisted of a glass reactor equipped with a magnetic stirrer and a reflective base to enhance light distribution. The distance between the light source and the solution surface was fixed at 20 cm. In a typical experiment, 0.4 g of catalyst was dispersed in 400 mL of MB solution with an initial concentration of 10 mg.L^{-1}. Prior to light irradiation, the suspension was magnetically stirred in the dark for 30 min to establish adsorption–desorption equilibrium. The suspension was then exposed to light irradiation under continuous stirring.

Figure 1. Model of photocatalytic reactor.

At predetermined time intervals, aliquots were withdrawn, centrifuged (DSC158T, Taiwan) to remove catalyst particles. The residual MB concentration was subsequently analyzed using a UV-Vis spectrophotometer (Shimadzu UV-2600) at a wavelength of 663 nm. The photocatalytic performance was expressed as the ratio C_t/C_0, and the degradation efficiency was calculated according to Eq. (1):

$$\eta(\%) = \frac{C_0 - C_t}{C_0} \times 100 \quad (1)$$

The effects of catalyst dosage, solution pH, and initial MB concentration were further investigated to evaluate the influence of key photocatalytic performance.

Catalyst stability was evaluated through repeated cycles (90 min per cycle). After each cycle, the catalyst was recovered by centrifugation, thoroughly washed several times with deionized water, dried at 100 °C, and reused under identical conditions. All photocatalytic experiments were conducted in triplicate under identical experimental conditions. The reported values represent the mean of three independent measurements. Error bars shown in the figures represent ± one standard deviation from the mean values.

3. Results and Discussion

3.1. Structural and Morphological Properties

The morphology and elemental composition of the vermiculite and the synthesized TiO_2/vermiculite composites were analyzed by SEM and EDX, as presented in Figure 2. The pristine vermiculite (Figure 2a) exhibits a typical layered and plate-like structure characteristic of 2:1 phyllosilicate mineral [11,21]. This lamellar architecture provides a robust mechanical framework and an expansive surface area, which is ideal for the effective immobilization of TiO_2 nanoparticles [5]. Furthermore, these silicate layers serve as a physical barrier that mitigates the aggregation of nanoparticles, a common drawback observed in unsupported TiO_2 powders [5,22].

Following TiO_2 loading and calcination at 450 °C, significant morphological transformations are observed (Figure 2b). Uniformly dispersed spherical TiO_2 nanoparticles are clearly visible, firmly anchored to the vermiculite flakes, resulting in a significantly rougher and more heterogeneous surface compared to the pristine vermiculite. This high degree of dispersion corroborates the "skeletal effect" provided by the vermiculite matrix, as discussed by Han *et al.* [11] and Szczepanik [21], which maintains the nanoscale dimensions of the catalyst and maximizes the availability of active sites for the degradation of organic pollutants [18,23].

The EDX spectrum (Figure 2c) confirms the presence of Ti and O elements, in addition to the characteristic mineral constituents of vermiculite, including Si, Al, Mg, K, and Fe [24]. The emergence of high-intensity Ti signals directly verifies the successful integration of TiO_2

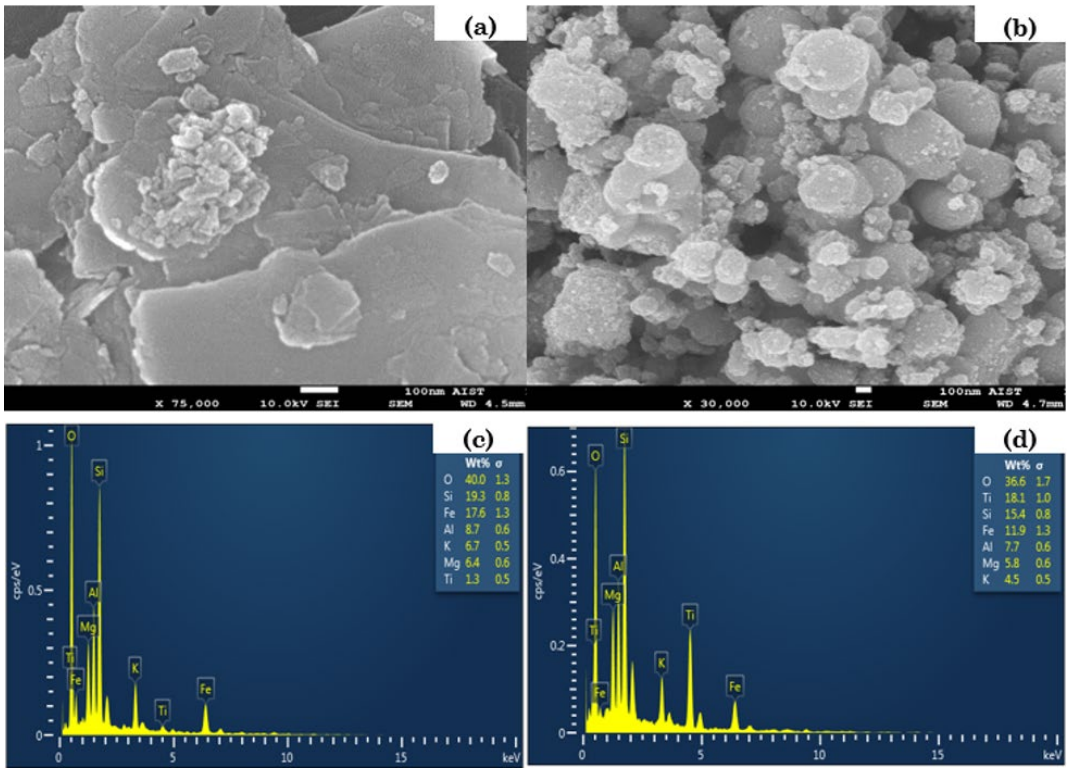

Figure 2. SEM images and EDX spectra of vermiculite (a, c) and TiO_2/ver (450 °C) (b, d).

onto the support via the sol-gel process. According to Dlamini *et al.* [5], this interaction often involves the formation of Ti-O-Si chemical bonds, which help stabilize the active photocatalytic phase and improve charge transfer kinetics at the mineral-semiconductor interface [11,25].

As calcination temperatures increase further, previous studies indicate that thermal sintering becomes a dominant factor, leading to crystal growth and particle agglomeration [19,23]. This morphological evolution typically results in the collapse of the porous structure and a reduction in specific surface area, which negatively impacts the reaction kinetics and overall photocatalytic performance of the composite [18].

The crystalline structure of the synthesized materials was characterized using XRD, as shown in Figure 3. The pristine vermiculite displays characteristic diffraction peaks of layered silicate minerals, with a prominent peak at 2θ = 26.5°, indicating that the support structure integrity of the support framework is maintained following the initial treatment steps [5]. For the commercial TiO_2 (P25), distinct diffraction peaks corresponding to the anatase phase are observed at 2θ = 25.3° (101), 37.8° (004), 48.0° (200), 54.2° (105), and 62.8° (204) [22].

For the TiO_2/Ver composites, the simultaneous presence of diffraction peaks from both TiO_2 and vermiculite confirms the successful formation of the composite without complete destruction of the support structure. In the V-450 sample, the anatase diffraction peaks are clearly observed with relatively high intensity, whereas the characteristic peaks of vermiculite remain detectable, indicating that the support structure was maintained after calcination at 450 °C [22].

As the calcination temperature increases to 600 °C (V-600), the material remains predominantly in the anatase phase. However, the diffraction peaks become significantly sharper and narrower [18]. This evolution serves as evidence for improved crystallinity and crystallite growth driven by the increased thermal energy input [18]. Concurrently, a slight reduction in the intensity of vermiculite peaks is observed, which may be attributed to the dense surface coverage by TiO_2 or localized structural rearrangement within the silicate layers [25].

At 800 °C (V-800), the peak of rutile phase becomes evident, indicating partial anatase to rutile transformation at elevated temperature [22]. This phase transformation is typically accompanied by crystallite growth, particle agglomeration, and a reduction in specific surface area [5]. These structural changes are known to adversely affect photocatalytic performance by decreasing the number of accessible active sites and limiting adsorption capacity [21].

Comparative analysis highlights that the calcination temperature is a decisive factor governing the structural evolution of the composites [22]. At lower temperature (450 °C), TiO_2 exists predominantly in the anatase phase with smaller crystallite size, which is recognized for its superior photocatalytic activity due to its

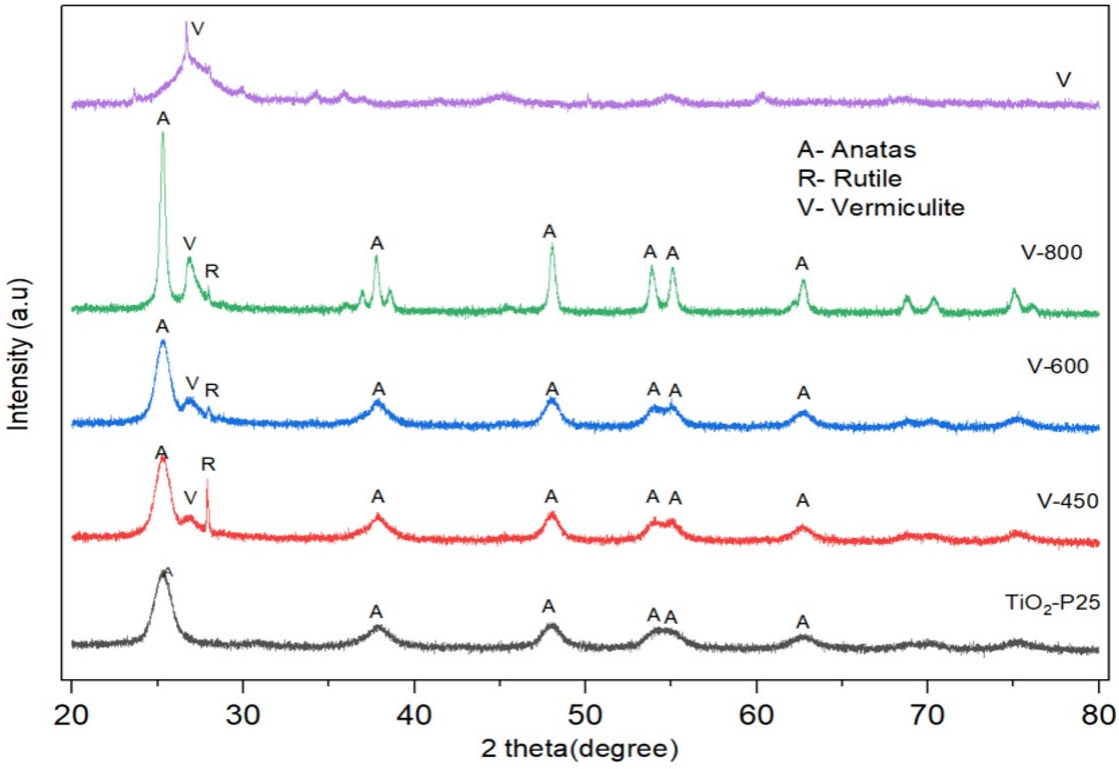

Figure 3. XRD pattern of sample.

favorable electronic band structure and its enhanced ability to suppress electron-hole recombination compared to the rutile phase [26].

Overall, the XRD analysis indicates that the V-450 sample possesses the most optimal crystalline structure, maintaining the highly active anatase phase while minimizing rutile formation and excessive crystallite growth [22]. This structural advantage provides a strong basis for explaining the superior photocatalytic performance of this sample compared to those calcined at higher temperatures.

The FT-IR spectra of TiO_2, vermiculite (Ver) and the TiO_2/ver composite calcined at 450 °C (V-450) are shown in Figure 4. For vermiculite, the broad absorption band centered at approximately 3400 cm^{-1} and the weak band at 1630 cm^{-1} are attributed to the stretching and bending vibrations of hydroxyl groups (-OH) and adsorbed water molecules, respectively [11,21]. The intense signal in the 1000-1100 cm^{-1} region corresponds to the Si-O stretching vibration of the silicate framework, confirming the characteristics layered aluminosilicate structure of vermiculite [11].

Pure TiO_2 displays characteristics absorption bands below 800 cm^{-1}, which are assigned to Ti-O-Ti lattice vibrations [21], In the V-450 composite, the simultaneous presence of Si-O and Ti-O-Ti bands confirms the successful immobilization of TiO_2 onto the support. Notably, the Si-O stretching band shifts from 985.9 cm^{-1} in the raw vermiculite to a higher wavenumber (1002.1 cm^{-1}). This red shift provides critical evidence for the formation of Si-O-Ti chemical bonds via condensation reactions between the surface hydroxyl groups of the mineral and the titanium precursor [11]. Such interfacial bonding not only ensures the uniform dispersion of nanoparticles but also creates effective charge-transfer channels at the mineral-semiconductor interface, which is essential for enhancing photocatalytic efficiency [11].

The textural properties of the materials are summarized in Table 1. The pristine vermiculite exhibits a relatively low specific surface area (9.04 $m^2.g^{-1}$), consistent with its compact, stacked layered morphology [18]. After TiO_2 loading, the surface area increases significantly to 105.78 $m^2.g^{-1}$ for the V-450 sample, signifying the successful formation of nanosized TiO_2 particles and the development of a well-defined mesoporous structure [11].

With increasing calcination temperature, the surface area decreases progressively from 105.78 $m^2.g^{-1}$ (V-450) to 81.68 $m^2.g^{-1}$ (V-600) and 65.7 $m^2.g^{-1}$ (V-800). This reduction can be attributed to

Table 1. Textural properties of TiO_2/vermiculite composites calcined at different temperatures.

Sample	BET surface area ($m^2.g^{-1}$)	Pore volume (cm^3/g)		Pore size (nm)	
		Adsorption	Desorption	Adsorption	Desorption
TiO_2-P25	136.96	0.787	0.788	17.98	16.59
V-450	105.78	0.254	0.285	7.70	8.00
V-600	81.68	0.215	0.235	8.82	9.31
V-800	65.7	0.197	0.205	9.87	10.14
Vermiculite	9.04	0.039	0.55	16.2	19.64

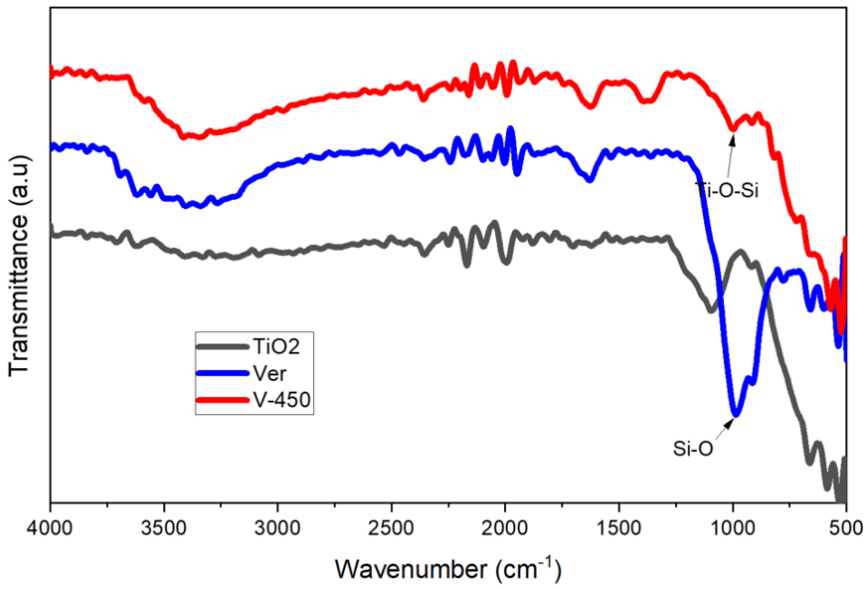

Figure 4. FT-IR spectra of TiO_2, Ver and V-450.

thermally induced sintering, crystallite growth, and partial collapse of the porous structure [21]. In parallel, the pore volume decreases, while the average pore diameter increases from 77.0 to 98.7 Å, suggesting the coalescence of smaller mesopores into larger voids as the temperature rises. These structural transformations indicate that while higher calcination temperatures improve crystallinity (as shown in XRD results), they simultaneously deteriorate the textural properties that are vital for active photocatalytic sites [5,21].

3.2. Photocatalytic Activity

3.2.1. Investigation of the photocatalytic activity of TiO_2 catalysts

The photocatalytic degradation of methylene blue (MB) is presented in Figure 5a. Pristine vermiculite exhibits limited removal efficiency, which can be primarily attributed to physical adsorption [11]. In contrast, all TiO_2-loaded composites demonstrated significant enhanced activity, confirming the successful integration of the semiconductor phase. Among the samples, V-450 exhibits the highest performance, achieving a degradation efficiency of 57.6% within 15 min and nearly complete removal (≈100%) after 90 min of irradiation.

All photocatalytic experiments were conducted in triplicate, and the relatively small error bars shown in Figure 5a indicate good reproducibility of the experimental results. This optimized activity is attributed to a critical balance possesses a high specific surface area (105.78 m^2/g) and a pure anatase phase, which is widely recognized for its superior ability to suppress electron-hole recombination compared to the rutile phase [22]. Furthermore, the presence of Si-O-Ti chemical bonds at the interface (suggests by FT-IR) facilitates a synergistic "adsorption-photodegradation" cycle [11]. In this mechanism, the vermiculite support acts as a molecular "enrichment matrix", pre-concentration MB molecules near the TiO_2 active sites, thereby accelerating the surface reaction kinetics [19].

As the calcination temperature increases to 600 °C (V-600) and 800 °C (V-800), the degradation efficiency decreases noticeably, reaching only 49.7% and 45.6% after 15 min, and 97.9% and 92.1% after 90 min, respectively. This deterioration in performance is linked to thermally induced sintering and the partial transformation of anatase to the less active rutile phase [21]. The reduction in specific surface area and the collapse of mesopores at elevated temperatures (as shown in Table 1) significantly decreases the density of accessible active sites and hinders the mass transfer of reactants [23].

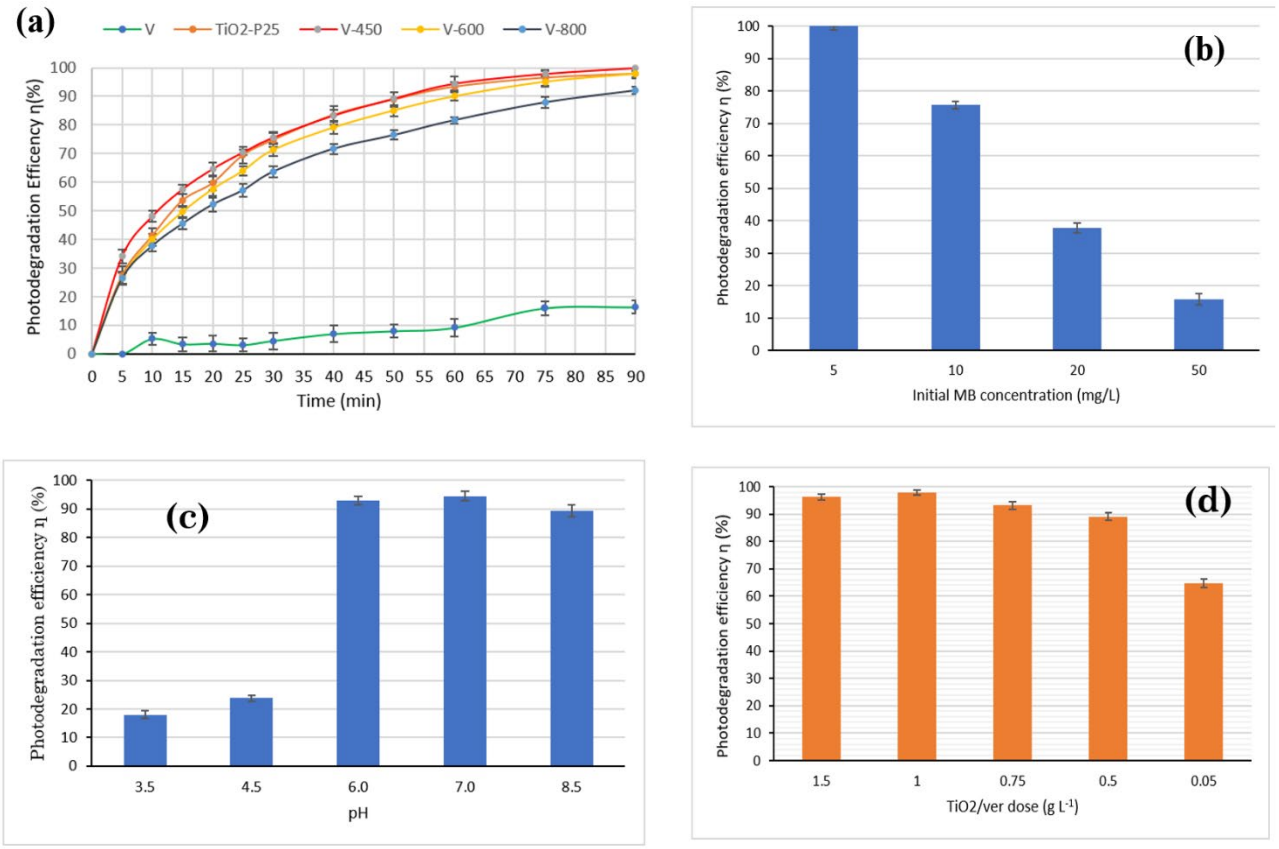

Figure 5. Photocatalytic degradation of methylene blue: (a) effect of catalyst type, (b) initial MB concentration, (c) pH, and (d) catalyst dosage.

3.2.2. Investigating the factors affecting the efficiency of catalysts

The effects of initial MB concentration, solution pH and catalyst dosage on the photocatalytic degradation efficiency of MB over the V-450 catalyst are presented in Figure 5b-d. Effect of initial pollutant concentration as illustrated in Figure 5b, the degradation efficiency declined sharply as the initial MB concentration increased from 5 to 50 mg.L^{-1}. At a low concentration (5 mg.L^{-1}), nearly 100% removal was achieved, whereas at 50 mg.L^{-1}, the efficiency dropped to 15.7%. This trend is consistent with findings by Kiwaan *et al.* [27]. This reduction can be attributed to active site saturation and reduced light penetration caused by the increased optical density of the solution at higher MB concentrations [11,28].

The effect of solution pH (Figure 5c) highlights the importance of electrostatic interactions at the catalyst-pollutant interface. The efficiency was lowest in acidic condition (pH of 3.5-4.5) and reached a maximum near neutrality (pH of 6-7). The enhanced photocatalytic activity under near-neutral conditions is associated with more favorable adsorption behavior and improved generation of reactive oxidative species [4].

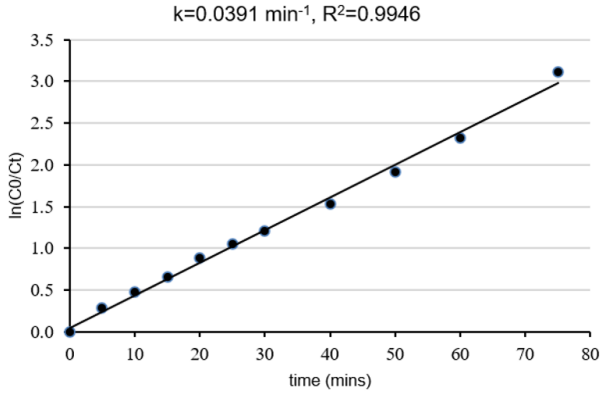

Figure 6. The kinetic curves of V-450 (Initial MB concentration of 10 mg.L^{-1}, solution pH of 7, and catalyst dosage of 1.0 g.L^{-1}).

As shown in Figure 5d, increasing the catalyst dosage from 0.05 to 1.0 g.L^{-1} significantly improved the degradation efficiency from 64.7% to 97.8% due to the increased availability of photocatalytic active sites. However, a slight decrease in efficiency (96.3%) was observed at 1.5 g, likely because excessive catalyst loading increased suspension turbidity and light scattering, thereby limiting photon penetration [17].

The reaction kinetics for the degradation of MB over the V-450 were evaluated using pseudo-first-order Langmuir-Hinshelwood (L-H) model, which is the standard framework for describing surface mediated photocatalytic processes at low pollutant concentration [1]. The model is expressed as:

$$\ln\left(\frac{C_0}{C_t}\right) = kt \quad (2)$$

where C_0 and C_t are the MB concentration at irradiation times $t = 0$ and t, respectively, and k (min^{-1}) is the rate reaction.

As shown in Figure 6, a strong linear correlation between ln $(C_0/C_t)$and irradiation time was obtained within the range of 0–75 min interval ($R^2 = 0.9946$). The apparent rate constant for V-450 was determined to be k = 0.0391 min^{-1}. This high degree of linearity confirms that under the applied conditions, the degradation process is primarily governed by surface reaction kinetics rather than mass transfer limitations [4]. The superior rate constant obtained for V-450 is a direct consequence of the structural optimizations discussed in Sections 3.1 and 3.2.1. To further contextualize the superior photocatalytic efficiency of the V-450 composite, its performance was compared with recently reported/clay-based systems (Table 2).

The photocatalytic performance of the TiO_2/ver composite developed in this study was markedly superior, achieving nearly complete degradation of MB within 90 min of irradiation at an optimal catalyst dosage of 1 g.L^{-1}. Compared

Table 2. Comparison of the pollutant removal performance of V-450 and other already published (ND: Not defined).

Photocatalyst	Pollutant	Catalyst dosage (g/L)	Time (min)	Removal efficiency (%)	Rate constant, k (min^{-1})	Reference
TiO_2/ver (V-450)	MB	1	90	~100	0.0391	This study
Vt/g-C_3N_4/TiO_2	MB	0.75	60	99.33	ND	[17]
TiO_2/Kaolinite (TKCP80)	MB	ND	270	91.5	0.0097	[8]
TiO_2/Montmorillonite	MB	0.5	180	99.5	ND	[29]
g-C_3N_4/TiO_2/Hectorite	RhB	0.33	120	94.0	0.0171	[5]
TiO_2/EV	Drimaren Red	1.0	200	100	ND	[30]
TiO_2/SNLs (Vt)	MB	0.2	40	100	0.0153	[24]

with recently reported clay based photocatalytic systems, this result demonstrates highly competitive degradation kinetics. Specifically, Karunadasa *et al.* reported a TiO_2/kaolinite system with a constant rate (k) of only 0.0097 min^{-1}, which is approximately four times lower than that obtained for the V-450 sample in the present study [8]. Similarly, the rate constants reported for other clay supported photocatalysts, such as g-C_3N_4/TiO_2/hectorite (0.0171 min^{-1}) and TiO_2/SNLs derived from vermiculite (0.0153 min^{-1}), were also substantially lower than the value achieved in this work [5,24].

Notably, at the same catalyst dosage of 1 $g.L^{-1}$, the classical study by Machado *et al.* required up to 200 min to achieve complete pollutant conversion (100%) [29]. The reduction of the reaction time to only 90 min in the present study highlights the effectiveness of controlling the calcination temperature at 450 °C, which optimized the anatase crystalline phase while preserving a well-developed mesoporous structure with a high specific surface area (S_{BET} = 105.78 m^2/g).

3.2.3. Research on the catalyst's reusability

The reusability results, presented in Figure 7, indicate that the TiO_2/vermiculite composites maintain relatively stable photocatalytic activity over multiple cycles, with only a slight decline observed over time. This behavior demonstrates the good durability and operational stability of the synthesized materials.

The observed stability can be attributed to the effective immobilization of TiO_2 particles on the vermiculite surface, which helps reduce nanoparticle loss and aggregation during repeated photocatalytic cycles. In addition, the layered structure and inherent mechanical stability of vermiculite contribute to maintaining the structural integrity of the composite throughout successive reuse cycles [11,29]. These findings are consistent with previous studies, which have reported that TiO_2 immobilized on clay minerals or porous supports exhibits enhanced stability and reusability in aqueous pollutant degradation systems [12,19].

4. Conclusion

In this study, TiO_2/vermiculite composites were successfully synthesized via a sol–gel method and subsequently calcined at different temperatures to investigate the influence of thermal treatment on their structural characteristics and photocatalytic performance. The results demonstrated that calcination temperature significantly affected the structure, morphology, textural properties and photocatalytic activity of the synthesized composites. XRD analysis revealed that the anatase phase predominated in samples calcined at 450 and 600 °C, whereas partial anatase to rutile transformation occurred at 800 °C. SEM observations indicated increased particle growth and agglomeration with increasing calcination temperature. BET analysis further showed a progressive reduction in specific surface area and pore volume at elevated temperatures due to thermally induced sintering and pore collapse.

Among the investigated samples, V-450 exhibited the most favorable combination of structural and textural properties, including predominant anatase crystallinity and a relatively high specific surface area (105.78

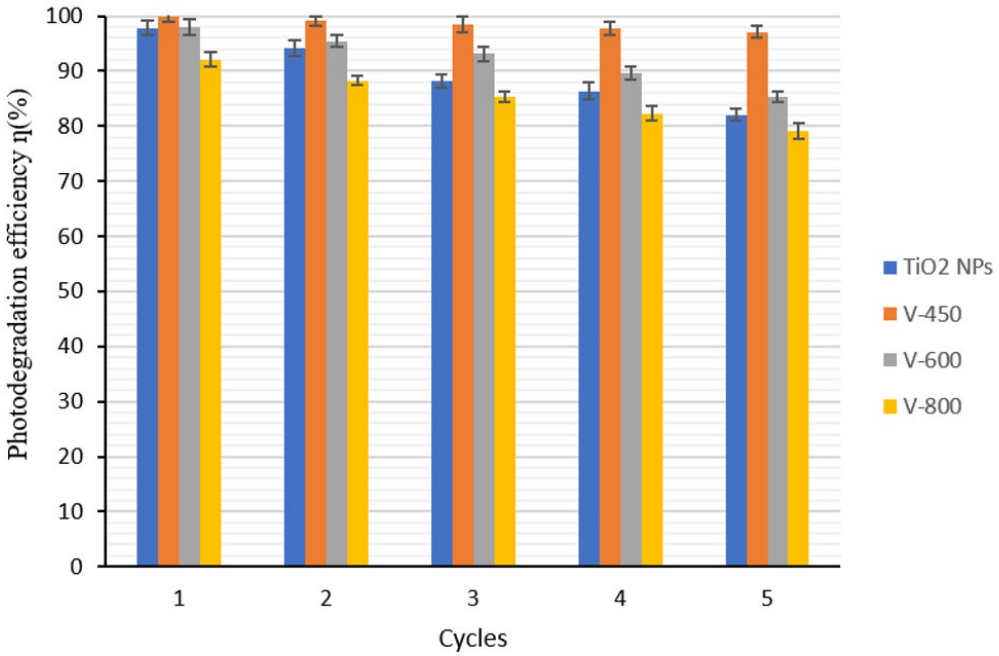

Figure 7. Reusability of commercial TiO_2 catalyst and synthesized TiO_2/vermiculite catalysts.

$m^2.g^{-1}$). Consequently, V-450 achieved complete degradation of methylene blue within 90 min under the optimal operating conditions of a catalyst dosage of 1.0 $g.L^{-1}$, an initial MB concentration of 10 $mg.L^{-1}$, and solution pH of 7. The degradation process followed pseudo-first-order kinetics with an apparent rate constant of 0.0391 min^{-1}. The catalyst also demonstrated satisfactory reusability over multiple photocatalytic cycles, indicating good operational stability. Overall, the results highlight the critical role of calcination temperature in governing the structure– activity relationship of TiO_2/ver composites and demonstrate the potential of vermiculite as a low-cost support material for TiO_2-based photocatalysts in wastewater treatment applications.

Acknowledgment

The authors declare that no external funding was received for this research.

CRedit Author Statement

Author Contributions: Ha Thi Thu Vu contributed to the conceptualization of the study, research planning, design of photocatalyst synthesis experiments, and revision and finalization of the manuscript. Nam Duy Dao contributed to the conceptualization of the study, research planning, design of photocatalytic activity experiments, data analysis and interpretation, manuscript writing, and manuscript revision. Trang Vu Minh performed the experiments and contributed to manuscript revision. Hai Trung Huynh provided supervision, scientific comments, and suggestions to improve both the research and the manuscript. All authors have read and agreed to the published version of the manuscript.

References

[1] Chauke, N.M., Ngqalakwezi, A., Raphulu, M. (2025). Transformative advancements in visible-light-activated titanium dioxide for industrial wastewater remediation. *International Journal of Environmental Science and Technology*, 22, 8521–8552. DOI: 10.1007/s13762-025-06397-2.

[2] Cozzolino, V., Coppola, G., Calabrò, V., Chakraborty, S. (2025). Heterogeneous TiO_2 photocatalysis coupled with membrane technology for persistent contaminant degradation: A critical review. *Applied Water Science*, 15(9), Article 97. DOI: 10.1007/s13201-025-02493-3.

[3] Dao, D.N., Cao, T.H.H., Nghiem, M.H., Van, D.A., Ha, V.H., Vu, M.T., Vu, Q.M., Nguyen, B.N., Vu, T.T.H., Huynh, T.H. (2024). Study on the Application of a Photocatalytic Titanium Dioxide Coating on Glass Beads for the Treatment of Perfluorooctane Sulfonic Acid. *Journal of Chemistry*, 2024, 5516249. DOI: 10.1155/2024/5516249.

[4] Danfá, S., Martins, R.C., Quina, M.J., Gomes, J. (2021). Supported TiO_2 in ceramic materials for the photocatalytic degradation of contaminants of emerging concern in liquid effluents: A review. *Molecules*, 26(17), 5363. DOI: 10.3390/molecules26175363.

[5] Dlamini, M.C., Maubane-Nkadimeng, M.S., Moma, J.A. (2021). The use of TiO_2/clay heterostructures in the photocatalytic remediation of water containing organic pollutants: A review. *Journal of Environmental Chemical Engineering*, 9(6), 106546. DOI: 10.1016/j.jece.2021.106546.

[6] Vu, T.H.T., Lam, T.T., Dao, D.N., Van, D.A., Huynh, T.H. (2023). A Composite of TiO_2 Quantum Dots and TiO_2 Nanoparticles Coated on Anti-Bumping Glass Beads (TiO_2QDs–TiO_2NPs/GBs), with a Very Low Content of TiO_2 as a High Performance Photocatalyst. *Journal of Chemistry*, 2023, 3400175. DOI: 10.1155/2023/3400175.

[7] Swaminaathan, P., Saravanan, A., Yaashikaa, P.R., Vickram, A.S. (2024). Recent advances in photocatalytic degradation of persistent organic pollutants: Mechanisms, challenges, and modification strategies. *Sustainable Chemistry for the Environment*, 8, 100171. DOI: 10.1016/j.scenv.2024.100171.

[8] Karunadasa, K.S.P., Wijekoon, A.S.K., Manoratne, C.H. (2024). TiO_2-kaolinite composite photocatalyst for industrial organic waste decontamination. *Next Materials*, 3, 100065. DOI: 10.1016/j.nxmate.2023.100065.

[9] Cardona, Y., Korili, S.A., Gil, A. (2024). Use of clays and pillared clays in the catalytic photodegradation of organic compounds in aqueous solutions. *Catalysis Reviews*, 66(5), 2063–2110. DOI: 10.1080/01614940.2023.2178736.

[10] Napruszewska, B.D., Duraczyńska, D., Kryściak-Czerwenka, J., Nowak, P., Serwicka, E.M. (2024). Clay Minerals/TiO_2 Composites—Characterization and Application in Photocatalytic Degradation of Water Pollutants. *Molecules*, 29, 4852. DOI: 10.3390/molecules29204852.

[11] Han, L., Yue, X., Wen, L., Zhang, M., Wang, S. (2023). A Novel Vermiculite/TiO_2 Composite: Synergistic Mechanism of Enhanced Photocatalysis towards Organic Pollutant Removal. *Molecules*, 28(17), 6398. DOI: 10.3390/molecules28176398.

[12] Fendi, K., Bouzidi, N., Boudraa, R., Saidani, A., Manseri, A., Eliche-Quesada, D., Nguyen Hai, T., Bollinger, J.C., Salvestrini, S., Kebir, M., Belkessa, N., Mouni, L. (2024). Testing of Kaolinite/TiO_2 Nanocomposites for Methylene Blue Removal: Photodegradation and Mechanism. *International Journal of Chemical Reactor Engineering*, 22(12), 1493–1508. DOI: 10.1515/ijcre-2024-0145.

[13] Li, L., Liu, Y., Zhang, H., Shen, H., Yin, X., Li, H., Peng, H., Zhou, S., Liu, Y. (2025). TiO_2-loaded halloysite nanocomposites: Achieving the UV resistance and dielectric stability of polyurea. *Polymer Degradation and Stability*, 241, 111549. DOI: 10.1016/j.polymdegradstab.2025.111549.

[14] Vu, V.T., Nguyen, T.H., Hoang, M.T., Nguyen, D.V., Tran, V.A., Dinh-Trinh, T., Nguyen, T.T.H. (2026). Synthesis of Fe-, Co-Doped Vermiculite for Enhanced Antibiotic Adsorption and Photocatalytic Degradation. *Case Studies in Chemical and Environmental Engineering*, 13, 101305. DOI: 10.1016/j.cscee.2025.101305.

[15] Xing, Z., Zhang, J., Cui, J., Yin, J., Zhao, T., Kuang, J., Zhou, W. (2018). Recent Advances in Floating TiO_2-Based Photocatalysts for Environmental Application. *Applied Catalysis B: Environmental*, 225, 452–467. DOI: 10.1016/j.apcatb.2017.12.005.

[16] Nguyen, T.H., Chu, V.H., Vu, V.T., Nguyen, X.D., Luu, V.H., Nguyen, M.N. (2025). Floating Photocatalyst Based on Fe-Doped TiO_2 Immobilized on Vermiculite for Degradation of Ciprofloxacine. *Vietnam Journal of Science and Technology*, 63(1), 111–122. DOI: 10.15625/2525-2518/19250.

[17] Fu, Q., Tan, F., Wu, Y. (2024). Preparation of vermiculite/g-C_3N_4/TiO_2 composites and their degradation of dye wastewater. *Polyhedron*, 247, 116713. DOI: 10.1016/j.poly.2023.116713.

[18] Kim, M.G., Kang, J.M., Lee, J.E., Kim, K.S., Kim, K.H., Cho, M., Lee, S.G. (2021). Effects of Calcination Temperature on the Phase Composition, Photocatalytic Degradation, and Virucidal Activities of TiO_2 Nanoparticles. *ACS Omega*, 6(16), 10668–10678. DOI: 10.1021/acsomega.1c00043.

[19] Zhang, J., Wen, X., Yang, X., Chen, C., Cheng, F. (2024). Effect of Calcination Temperature of Titanium Dioxide (TiO_2) on Adsorption Performance of Doxycycline Hydrochloride. *Desalination and Water Treatment*, 317, 100113. DOI: 10.1016/j.dwt.2024.100113.

[20] Chau, J.H.F., Lai, C.W., Leo, B.F., Juan, J.C., Lee, K.M., Badruddin, I.A., Kumar, A., Sharma, G. (2025). Study of Calcination Temperature Influence on Physicochemical Properties and Photodegradation Performance of Cu_2O/WO_3/TiO_2. *Catalysts*, 15(6), 601. DOI: 10.3390/catal15060601.

[21] Szczepanik, B. (2017). Photocatalytic Degradation of Organic Contaminants over Clay-Nanocomposites: A Review. *Applied Clay Science*, 141, 227–239. DOI: 10.1016/j.clay.2017.02.029.

[22] Swathi, K.S., Naik, K.G. (2026). Calcination Effect on the Properties of Sol–Gel Synthesized TiO_2 Nanomaterials. *Discover Industrial Chemistry Materials*, 1, 3. DOI: 10.1007/s44508-026-00003-0.

[23] Jin, L., Dai, B. (2012). TiO_2 Activation Using Acid-Treated Vermiculite as a Support: Characteristics and Photoreactivity. *Applied Surface Science*, 258(8), 3386–3392. DOI: 10.1016/j.apsusc.2011.11.017.

[24] Wang, L., Wang, X., Cui, S., Fan, X., Zu, B., Wang, C. (2013). TiO_2 Supported on Silica Nanolayers Derived from Vermiculite for Efficient Photocatalysis. *Catalysis Today*, 216, 95–103. DOI: 10.1016/j.cattod.2013.06.026.

[25] Chong, M.N., Vimonses, V., Lei, S., Jin, B., Chow, C., Saint, C. (2009). Synthesis and Characterisation of Novel Titania Impregnated Kaolinite Nano-Photocatalyst. *Microporous and Mesoporous Materials*, 117(1–2), 233–242. DOI: 10.1016/j.micromeso.2008.06.039.

[26] Nguyen, T.H., Nguyen, T.H., Vu, A., Minh, T.L. (2025). Photocatalytic Degradation of Methyl Orange Using TiO_2-Coated Cordierite Substrates: A Comparison of Dip-Coating and Spray-Coating Methods. *Bulletin of Chemical Reaction Engineering & Catalysis*, 20(4), 594–606. DOI: 10.9767/bcrec.20400.

[27] Kiwaan, H.A., Atwee, T.M. (2020). Photocatalytic degradation of organic dyes in the presence of nanostructured titanium dioxide. *Journal of Molecular Structure*, 1200, 127115. DOI: 10.1016/j.molstruc.2019.127115.

[28] Fujishima, A., Zhang, X., Tryk, D.A. (2008). TiO_2 Photocatalysis and Related Surface Phenomena. *Surface Science Reports*, 63(12), 515–582. DOI: 10.1016/j.surfrep.2008.10.001.

[29] Zeng, L., Sun, H., Peng, T., Lv, X. (2019). Comparison of the Phase Transition and Degradation of Methylene Blue of TiO_2, TiO_2/Montmorillonite Mixture and TiO_2/Montmorillonite Composite. *Frontiers in Chemistry*, 7, 538. DOI: 10.3389/fchem.2019.00538.

[30] Machado, L.C.R., Torchia, C.B., Lago, R.M. (2006). Floating Photocatalysts Based on High Surface Area Exfoliated Vermiculite for Water Decontamination. *Catalysis Communications*, 7(8), 538–541. DOI: 10.1016/j.catcom.2005.10.020.